

# Dielectric Constants of Single-Wall Carbon Nanotubes at Various Frequencies

Yan-Huei Li<sup>1</sup> and Juh-Tzeng Lue<sup>2,\*</sup>

<sup>1</sup>Department of Electrical Engineering and <sup>2</sup>Department of Physics

A cylindrical rod composed of a uniform mixture of single-wall carbon nanotubes and alumina powders dissolved in paraffin was inserted in the center of a radio frequency cavity. The complex dielectric constant of carbon tubes at various frequencies was measured by a resistance-inductance-capacitance (RLC) meter and a microwave network analyzer. The cylindrical rod benefits the protection of the sample from adsorbing moisture and preventing the rod from filling with air, thus making accuracy experiment values. The real part and the imaginary part of the dielectric constants of single-wall carbon nanotubes are, respectively, increase and decrease in magnitudes as frequency increases satisfactorily in complying with the portray from the free electron Drude model.

**Keywords:** Dielectric Constants from DC to Microwave Frequencies, Single Wall Carbon Nanotubes, Cylindrical Resonator.

## 1. INTRODUCTION

In 1991,<sup>1</sup> Iijima first observed multi-wall carbon nanotubes (MWCNT) which are rolls of multiple graphene sheets with outside diameters of 10 ~ 20 nm. Two years later, Iijima<sup>2</sup> and Bethune<sup>3</sup> discovered single-wall carbon nanotubes (SWCNT) with diameters of 1 ~ 3 nm. The crystallographs are usually defined by the two dimensional chiral vector  $C_h$ , which can be decomposed into the unit vectors  $\vec{a}$  and  $\vec{b}$  of the basic benzene cells by  $\vec{C}_h = n\vec{a} + m\vec{b}$  where  $m$ ,  $n$  are integers. The single-wall CNT behaves metallic or semiconducting depending on whether  $m - n = 3q$  or not, where  $q$  is an integer. Four electrons interacting between two channels within the unit cell of CNTs implying two units of quantum conductance  $G = 2G_0 = 4e^2/h$  result in a resistivity of 4.2 k $\Omega$  (Ref. [4]) for SWCNT and 190 k $\Omega$  for MWSCNT,<sup>5</sup> respectively. Detailed analysis at low temperatures illustrated the SWCNT has a long-range electron density function inheriting with the 1D Luttinger liquid conducting transport.<sup>6</sup> In succinct, owing to the low density of states, the conduction transport of SWCNT approaches to be ballistic, in which the electron moves without occurring scattering with impurities or phonons.

The dielectric constants of CNTs decisively determine their pragmatic applications in electro optics, while have rarely been reported because of their high absorption to electromagnetic waves and so tiny to be measured by traditional method. The high microwave-field absorption of the

metallic SWCNTs excludes employing conventional methods by inserting a powder-pressed thin disk in a microwave guide to determine the dielectric constant just by measuring the attenuation and phase delay of the penetrated waves. In our previous works,<sup>7,8</sup> we have proposed a novel method of measuring the dielectric constants of metallic nanoparticles by using a microwave dielectric resonator. The metallic nanoparticles were mixed with alumina powder and paraffin to form a rod. The resonant frequency and  $Q$  factor were measured at the spectral  $TM_{010}$  mode to derive the complex dielectric constant. Although spherical alumina particles can be closely stacked, whilst 30% of the volume in the pressed rod was still unfilled. This empty cells are usually occupied by water molecules in a humidity environment, resulting in a serious absorption of microwave fields. The microwave absorption due to moisture absorbed in the alumina powder and the air embedded in the particles adversely impacts the possibility for accurately determining the dielectric constants. Therefore the powder mixed with paraffin can disperse the absorption of moisture.

Dielectric constants specify the response of the dipole displacement in an external applied field in terms of ion and electron motions. Incident electromagnetic (EM) fields of different frequencies cause different responses from ions and electrons. As the size of the metal films or particles declines, the mean free path becomes constrained by surface scattering. Classical size effect,<sup>9</sup> which affects the dielectric constant, occurs as the metal film thickness or the particle size becomes smaller than or similar to, the

\* Author to whom correspondence should be addressed.

mean free path  $l$  of the carriers inside the metal. Quantum size effect arises as the particle size decreases further below the Bohr radius<sup>10,11</sup> where the continuous conduction band becomes discrete. The dielectric constants of nanosized SWCNTs closely controlled by the quantum size effect inheriting to their sizes, length, and structures.

## 2. MICROWAVE TM MODES AND THE Q FACTORS

A dielectric resonator (DR) that is composed of alumina powder with a high dielectric constant can significantly reduce the cavity volume and yield a high quality  $Q$ -factor. The construction detail of the DR is sketched in Figure 1 where a cylindrical rod of diameter  $b$  that comprises a mixture of metallic SWCNTs, alumina powder and paraffin with an effective dielectric constant  $\epsilon_2$  is installed into the center of a copper-made cavity that has an inner diameter  $d$ . The electromagnetic fields propagating inside the cavity can be solved from Maxwell's equations with proper boundary conditions. The  $TM_{010}$  mode has the advantages of a lowest resonant frequency that is independent of cavity length  $L$  and is easily identifiable. The  $TM_{010}$  mode is exploited because stronger electric fields are presented near the axis than those of the  $TE_{010}$  mode, resulting in a higher sensitivity on account of metallic absorption.

For a cylindrical cavity with a longitudinal coordinate along the  $z$  axis and having an azimuthal radius  $r$ , the resonant frequency for the  $TM_{010}$  mode can be solved from the boundary conditions to give the secular determinant<sup>12,13</sup>

$$\begin{vmatrix} J_0(s_2b) & -I_0(s_3b) & -K_0(s_3b) \\ \frac{\epsilon_2}{s_2} J'_0(s_2b) & \frac{\epsilon_3}{s_3} I'_0(s_3b) & \frac{\epsilon_3}{s_3} K'_0(s_3b) \\ 0 & I_0(s_3d) & K_0(s_3d) \end{vmatrix} = 0 \quad (1)$$

where

$$s_2 = \omega \sqrt{\mu \epsilon_2} = \sqrt{-\left(\frac{p\pi}{L}\right)^2 + (2\pi f)^2 \mu \epsilon_2}$$

$$s_3 = \omega \sqrt{\mu \epsilon_3} = \sqrt{\left(\frac{p\pi}{L}\right)^2 - (2\pi f)^2 \mu \epsilon_3}$$

$$h^2 = (j\beta)^2 + \omega^2 \mu \epsilon, \quad \text{and} \quad \beta = \frac{p\pi}{L}, \quad h_3 = js_3$$

The  $m$ -th order Bessel functions are in forms of  $J_m(sr)$  and  $Y_m(sr)$  for  $h = s$ , and in forms of modified Bessel functions such as  $I_m(sr)$  and  $K_m(sr)$  for  $h = js$ . The final solutions of the EM fields within the dielectric rod (for  $r < b$ ) and between the air space ( $b < r < d$ ) of the cavity are, respectively [14]:

for  $r < b$ ,

$$E_{z2} = C_2 J_0(s_2 r) \quad (2)$$

for  $b < r < d$ ,

$$E_{z3} = (C_2 X) J_0(s_3 r) + (C_2 Y) Y_0(s_3 r) \quad (3)$$

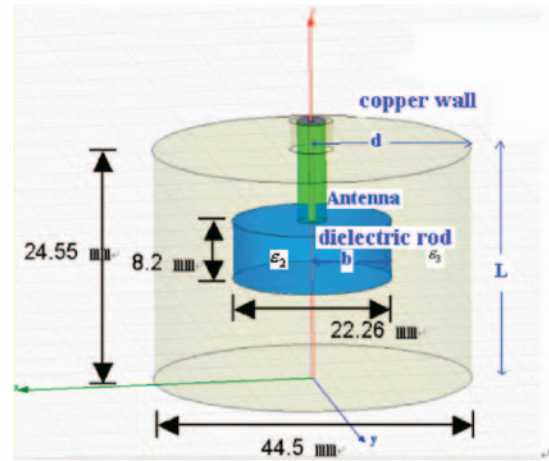


Fig. 1. The dimensions of the cylindrical cavity and sample rod.

In addition to the measurement of the resonant frequency to derive the real part of the dielectric constant  $\epsilon$ , we also measure the quality factor  $Q$  to derive the loss tangent and the imaginary part of  $\epsilon$ . The total energy stored in the cavity is

$$W_T = \frac{\epsilon_0 \epsilon_{r2}}{2} \int |E_{z2}|^2 dV_2 + \frac{\epsilon_0}{2} \int |E_{z3}|^2 dV_3 \quad (4)$$

where  $\epsilon_{r2}$  and  $\epsilon_0$  are the real parts of the dielectric constants of the inner rod and the outside air gap, respectively.

To measure the real and imaginary parts of the dielectric constants at low frequency alternate-current (ac), two metallic discs construction an RLC tank, we have

$$\epsilon_r = \frac{CL}{\epsilon_0 \pi R^2}, \quad \epsilon_i = \frac{\sigma}{\omega \epsilon_0} \quad (5)$$

$$\text{with } Q = \frac{wC}{G} = \frac{w\epsilon_r \epsilon_0}{\sigma}, \quad \epsilon_i = \frac{\epsilon_r}{Q} \quad (6)$$

where  $\sigma$  is the conductivity,  $C$  is the capacitance,  $L$  is the inductance,  $R$  is the resistance measured from the RLC meter. To immunize from radiation loss, the tank resonator was wrapped by an alumini foil.

The quality factors  $Q_0$  and  $Q_L$  are the unloaded cavity  $Q$  factors containing, respectively, without and with external wirings such as the transmission-line connector and the antenna. The  $Q_0$  can be expressed as

$$\frac{1}{Q_0} = \frac{P_c + P_d + P_{\text{SWCNT}} + P_r}{\omega \cdot W_r} = \frac{1}{Q_c} + \frac{1}{Q_d} + \frac{1}{Q_{\text{SWCNT}}} + \frac{1}{Q_r} \quad (7)$$

where  $Q_c$  is the conducting loss of the copper wall,  $Q_d$  is the dielectric loss from paraffin and alumina,  $Q_{\text{SWCNT}}$  is the loss from the SWCNTs, and  $Q_r$  is the radiation loss. The  $Q_L$  can be directly measured from the  $-3$  db position of the transmission spectra as given by  $Q_L = (f_0/f_2 - f_1)$ . The unloaded  $Q_0$  is simply derived from the formula<sup>15</sup> as  $Q_0 = \frac{Q_L}{1 - |S_{21}(f_0)|} = \frac{Q_L}{1 - 10^{-\text{IL}(\text{db})/20}}$ , where  $\text{IL}(\text{db})$  is the inserting loss, which can be directly read from the network analyzer.

The dielectric losses of the SWCNTs are given by

$$Q_{\text{SWCNT}} = \frac{\omega \times W}{P_{\text{SWCNT}}} = \frac{\omega \cdot \epsilon_0 \cdot \epsilon_{\text{eff}}}{\sigma \cdot f} = \frac{\epsilon_{\text{eff}}}{\epsilon_i \cdot f}$$

$$= \frac{W_T}{f W_2 \tan \delta_{\text{SWCNT}}} = \frac{W_T}{f W_2} \frac{\epsilon_{2r}}{\epsilon_{2i}} \quad (8)$$

where  $\epsilon_{2i}$  is the imaginary part of the effective dielectric constant, which is contributed mostly from SWCNTs. The  $Q_{\text{SWCNT}}$  can be derived from the difference of separated measurements including without and with metallic nanoparticles such as

$$\frac{1}{Q_{\text{SWCNT}}} \cong \frac{1}{Q_{02}} - \frac{1}{Q_{01}} \quad (9)$$

where  $Q_{01}$  and  $Q_{02}$  are defined for including without and with the SWCNTs.

### 3. DEDUCTION OF THE DIELECTRIC CONSTANT OF SWCNTs FROM SEVERAL COMPONENTS

The dielectric constant of SWCNTs is derived from the effective value of the total mixture by the effective medium approximation (EMA) as given by<sup>16</sup>

$$f_A \frac{\epsilon_A - \epsilon_{\text{eff}}}{\epsilon_A + 2\epsilon_{\text{eff}}} + f_B \frac{\epsilon_B - \epsilon_{\text{eff}}}{\epsilon_B + 2\epsilon_{\text{eff}}} + f_C \frac{\epsilon_C - \epsilon_{\text{eff}}}{\epsilon_C + 2\epsilon_{\text{eff}}} = 0 \quad (10)$$

where  $f_i$  and  $\epsilon_i$  are the volume ratio and dielectric constant of the  $i$ -th component, and  $\epsilon_{\text{eff}}$  is the effective value of the mixture. The EM fields are concentrated in the dielectric rod where the  $\epsilon$  of the alumina component is high. To retain the high quality factor, the volume ratio of SWCNTs should be below 1% otherwise the  $Q$  is too low to analyze the resonant spectrum.

The SWCNTs were purchased commercially from Shenzhen Nanotech Port Co., Limited with specifications of ranges of diameters: <2 nm; tube lengths: 5 ~ 15  $\mu\text{m}$ ; purity of carbons:  $\geq 90\%$ ; purity of SWCNTs: >80 %; ash contents:  $\leq 2$  wt%; special surface area: 600  $\text{m}^2/\text{g}$ , and amorphous carbons: <5%. The single wall was checked by the high-resolution transmission electron microscopy (HRTEM)<sup>17</sup> and the Raman spectroscopy as shown in Figures 2 and 3, respectively. The cross section view of the inset clearly shows the single-wall wrapped CNT. The graphite G band in the Raman spectrum is much stronger than the defect (D) band and the presence of the weak spectra at 100 ~ 300  $\text{cm}^{-1}$  as shown in Figure 3 both advocate features of single wall CNTs.

The sample rod, is prepared by first melting the paraffin in a mold to a desired inner diameter, from which, the mixed alumina and SWCNTs at a known weight ratio is poured and uniformly mixed in the mold. It is slowly cooled, then the cylindrical rod is extruded from the mold and is cut into a proper length. To exploit the effective

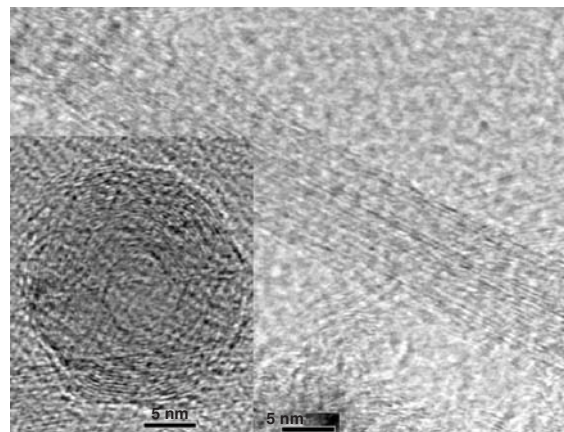


**Fig. 2.** The HRTEM showing the single wall carbon nanotube, the cross sectional view as sketched in the inset indicates the single wall wrapped CNT with a polygon at the other end.

medium theory, an accurate determination of the density of SWCNTs is required. We used the buoyancy method, by which a known weight of calcite was gradually poured into a glass filled with distilled water, in which a known weight of SWCNTs was embedded. When the densities of water and the SWCNTs become equal, the sunk CNTs will be floated. Repeat measurements yield a density of 1.37  $\text{g}/\text{cm}^3$  for this sample which strictly agrees with the theoretical calculation<sup>18</sup> expressing between 1.33 ~ 1.4  $\text{g}/\text{cm}^3$  for arm-chair, chiral and zigzag SWCNTs. Typical  $S_{21}$  transmission spectra were measured by an Anritsu 37347A network analyser.

### 4. RESULTS AND DISCUSSION

The densities of paraffin, alumina, and SWCNT are firstly determined to be 0.9021, 3.97, and 1.37  $\text{g}/\text{cm}^3$ , respectively, before applying the EMA theory. The  $\text{TM}_{010}$  mode is identified by which the characterizing resonance line does not shift when the cavity length is changed. The dielectric constants and the loss tangents of paraffin as derived from the resonant frequency and the  $Q$ -factor of the  $S_{21}$  spectra are  $2.268 \pm 0.004$  and  $2.0 \times 10^{-4}$ , respectively. Figures 4 and 5 provide the real and imaginary parts

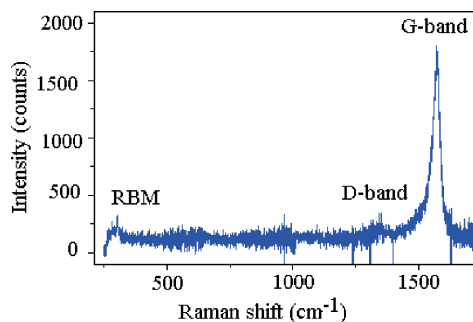


**Fig. 3.** The Raman spectrum showing the weak D-line and strong G-line, and the much weaker RBM lines for characterizing the SWCNTs.

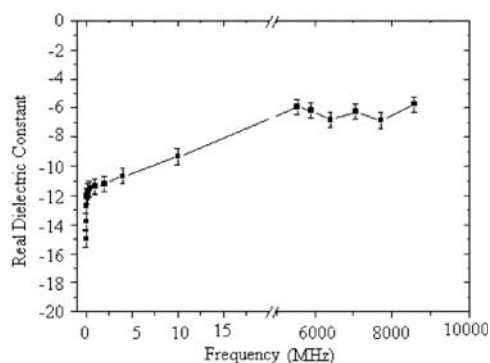


**Fig. 4.** The real parts of the dielectric constant for SWCNTs at various frequencies.

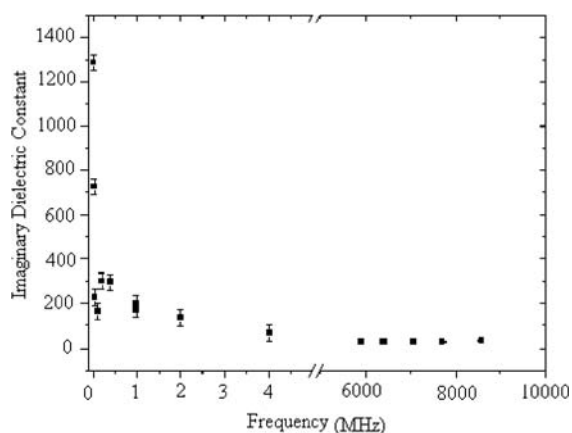


**Fig. 5.** The imaginary parts of the dielectric constant for SWCNTs at various frequencies.

of  $\epsilon$  for SWCNTs derived from the EMA theory for the rod composed of paraffin and alumina. The increase and decrease of the real and imaginary parts of the dielectric constant as the frequency increases are qualitatively follow the free electron Drude model.

To our knowledge, no data concern the dielectric constants of SWCNTs at microwave frequencies is available for comparison. In this work, a microwave dielectric resonator, which can be easily detached from the cavity for changing the mixture of SWCNTs and alumina powders was designed to measure the complex dielectric constant of SWCNTs from the resonant frequency and quality factors of its spectrum. It is still premature to identify a deterministic value of the dielectric constant of various kinds of CNTs, because it intimately depends

on the accurate determination of the numbers of wrapped sheets, radius, length, surface oxidation, and molecular defects. The microwave absorption crucially embodied in the metallic behavior of the material, making it extremely difficult to determine the imaginary part. The darkish appearance of many different metallic nanoparticles illustrates that the measured dielectric constants for CNTs, silver and iron nanoparticles, are close in proximity. Considering the unique specification of the material, we only report the measurement of the dielectric constant of SWCNTs and not for MWCNTs.

**Acknowledgments:** This work was supported by the National Science Council of the Republic of China under contract NSC 96-2112-M-007-001.

## References and Notes

1. S. Iijima, *Nature* 354, 56 (1991).
2. S. Iijima and T. Ichihashi, *Nature* 363, 603 (1993).
3. J. Bernholc, C. Brabec, M. B. Nardelli, A. Maiti, C. Roland, and B. I. Ya-Kobson, *Appl. Phys. A67*, 39 (1998).
4. C. T. White and T. N. Todorov, *Nature* 393, 240 (1998).
5. Z. H. Zhang, J. C. Peng, and H. Zhang, *Appl. Phys. Lett.* 79, 3515 (2001).
6. M. Bockrath, D. H. Cobden, J. Lu, A. G. Rinzler, R. E. Smalley, T. Balents, and P. L. McEuen, *Nature* 397, 598 (1999).
7. J. H. Liu, C. L. Chen, H. T. Lue, and J. T. Lue, *IEEE Microwave and Wireless Components Letters* 13, 181 (2003).
8. Y. S. Yeh, J. T. Lue, and Z. R. Zheng, *IEEE Trans. on Microwave Theory and Techniques* 53, 1756 (2005).
9. Y. S. Hor and J. T. Lue, *Appl. Phys. B62*, 303 (1996).
10. W. C. Huang and J. T. Lue, *J. Chem. Phys. Solids* 58, 1529 (1997).
11. W. C. Huang and J. T. Lue, *Phys. Rev. B* II-49, 17279 (1994).
12. H. T. Lue, J. T. Lue, and T. Y. Tseng, *IEEE Trans. on Instrum. Meas.* 51, 433 (2002).
13. D. K. Cheng, *Field and Wave Electromagnetic*, 2nd edn., Addison-Wesley, New York (1989), Ch. 7~10.
14. D. M. Pozar, *Microwave Engineering*, 2nd edn., Wiley, New York (1998).
15. B. W. Hakki and P. D. Coleman, *IEEE Trans. Microwave Theory Technol.* MTT-8, 402 (1960).
16. T. C. Choy, *Effective Medium Theory, Principles and Applications*, Oxford University Press, New York (1999).
17. Z. L. Wong and H. Chun, *Electron Microscopy of Nanotubes*, Kluwer Academic Publishers, Boston (2003), p.13.
18. G. Gao, T. Cagin, W. A. Goddard III, *Energetics, Structure, Mechanical and Vibration Properties of Single Walled Carbon Nanotubes (SWNT)*, *The Fifth Foresight Conference on Molecular Nanotechnology* (1997).

Received: 26 July 2006. Revised/Accepted: 24 January 2007.